The Seventh Asian-Pacific Symposium on Structural Reliability and Its Applications (APSSRA2020)
October 4–7 2020, Tokyo, Japan
T. Takada, I. Yoshida & T. Itoi (editors)

Characterization of Model Uncertainty for Necessary Face Pressures of Tunneling in Frictional Soils

Q. J. Pan[1], C. Tang[2], L. H. Zhao[3], and K. K. Poon[4]

[1] *Dept. of Civil and Environmental Engineering, National Univ. of Singapore, Singapore 117576. Email:panqiujing2013@gmail.com*
[2] *Dept. of Civil and Environmental Engineering, National Univ. of Singapore, Singapore 117576. Email: ceetc@nus.edu.sg*
[3] *Civil Engineering School, Central South University, Changsha, China 410075. Email: zhaolianheng@csu.edu.cn*
[4] *Dept. of Civil and Environmental Engineering, National Univ. of Singapore, Singapore 117576. kkphoon@nus.edu.sg*

Abstract: The face stability is a key issue in tunnel engineering, especially in weak grounds. This topic have attracted many researcher's attention and various theoretical models for predicting necessary face pressures against its failure were proposed in the light of the limit equilibrium method (LEM) and the kinematical approach of limit analysis method (LAM). Meanwhile, a large number of experimental studies have been conducted to study tunnel face stability. Using centrifuge testing results, this paper aims at applying Bayesian method to characterize the model uncertainties of three classical models of predicting limit face pressures in frictional soils, by incorporating the test uncertainties and parameter uncertainties. The obtained results show that the Mollon model is less biased than the other two; the Horn model tends to be conservative but its model uncertainty has the largest variability.

Keywords: model uncertainties, tunnel stability, limit face pressures, Bayesian analysis, centrifuge testing

1. Introduction

In order to deal with urban problems caused by rapid increase in population and decrease in land resources, tunnel constructions have become an efficient way for making use of urban underground space. One of the most important issues when digging a tunnel is the face stability. In closed-face tunneling by means of tunneling boring machines (TBM), shield machines can provide a continuous support with compressed air, excavated soils or bentonite slurry to the tunnel face, thus the support pressure is a key factor to govern the face stability. If the applied face pressures are not enough, the soils will move towards the tunnel face, eventually leading to surface subsidence.

Many researchers have developed simplified theoretical models to evaluate tunnel face stability, in the framework of the limit equilibrium method (LE) and the kinematical approach of limit analysis (LA). Both methods require an assumption of the failure mechanism of the tunnel face, based on which the LE and LA, respectively, considers the force equilibrium and the work rate balance. The construction of failure mechanisms is based on face failure features observed in experimental and numerical studies. The most classical failure mechanism in the context of the limit equilibrium method is the wedge-prism model (Horn 1961). With respect to the upper-bound limit analysis theory, one should cite the translational failure mechanism reported by Leca and Dormieux (1990) composing of a single or two conical blocks. It was improved by adding a series of truncated rigid blocks between the two conical blocks (Soubra et al. 2008, Mollon et al. 2009, Zhao et al. 2019), which allows the failure surface to move more freely. Given these translational failure mechanisms failed to cover the full tunnel face, Mollon et al. (2011) proposed a classical three-dimensional (3D) rotational failure mechanism generated by a spatial discretization technique. Assuming a cylindrical rotational velocity field, the 3D rotational failure mechanism is generated "point by point" instead of using existing standard geometric shapes such as cones or cylinders, which allows it to pose two significant characteristics: including the entire tunnel face and being consistent with the soil rotational movement observed in experiments. The 3D rotational failure mechanism has been shown to improve the existing kinematical solutions significantly in frictional soils with respect to translational mechanisms (Mollon et al. 2011).

These theoretical models are expected to give predictions that deviate from reality and differ in their precision comparing with experimental testing results, since they are an abstract representation of the tunnel face systems based on different assumptions for simplification. Thus these models are often subjected to model uncertainty. The model uncertainty may cause biased predictions and is important for geotechnical decision making (Phoon and Kulhawy 2005, Zhang et al. 2009, Zhang et al. 2015, Tang and Phoon 2018, Tang and Phoon 2019).

This paper aims to evaluate the model uncertainty of tunnel face pressures in frictional soils. Three representative models, namely the Horn's wedge-prism model, Soubra's multiple-block model and Mollon's 3D rotational model, are calibrated with using centrifuge experimental testing data. The Bayesian method is used to assess the model uncertainty by considering the parameter and test uncertainties.

2. Predictive models and centrifuge testing data

2.1 Predictive models

Three theoretical models of predicting necessary face pressures, the Horn model, Soubra model (Soubra et al. 2008) and Mollon model (Mollon et al. 2011), are considered in this study.

The Horn model consists of a sliding wedge ahead of the tunnel face and an overlaying prism up to the ground surface. The limit face pressure can be obtained by

equilibrating all forces acting on the wedge, including the vertical force obtained by applying the silo theory, the gravity of the wedge, the normal and shear forces acting on the inclined sliding surface, the face support forces. This model involves several user-defined parameters, such as the lateral stress coefficients in the sliding wedge and the prism, the distribution of vertical stresses inside the wedge, the assumptions of which lead to various variations. An overview of Horn's wedge-prism and its variations can be found in Zizka (2019). The version of Anagnostou and Kovári (1994) is adopted in this study.

The kinematical approach of limit analysis is able to provide an upper bound estimate to an active limit load, for instance the foundation capacity, or a lower bound to a reaction, such as the tunnel face pressure. In the Soubra's multiple-block model and Mollon's 3D rotational model, the limit face pressure can be obtained by equating the work rate of external forces, including the gravity and the face pressure, to the internal energy dissipation (Soubra et al. 2008, Mollon et al. 2011).

2.2 Centrifuge testing data

The stability of a tunnel face has been investigated by many researchers by means of experimental tests (Chambon and Corté 1994, Kamata and Mashimo 2003, Idinger et al. 2011, Chen et al. 2013, Lü et al. 2018, to cite a few). The centrifuge testing results performed by Chambon and Corté (1994) are employed to characterize the above predictive model uncertainties since the number of tests is large enough for Bayesian analysis on model uncertainty.

Chambon and Corté (1994) conducted a series of centrifuge experiments to study the face stability in cohesionless soils. The tunnel is modeled by a rigid metallic tube in diameter of 100mm. The model was accelerated to 50g and 100g (g=gravitational acceleration) in the experiments, respectively corresponding to prototype tunnels of 5.0m and 10m in diameter *D*. The soil cover depth to the tunnel diameter ratio *C*/*D* is set to change from 0.5 to 4.0. The Fontainebleau sand is used in the experiments. The unit weights of sands change from 15.3 kN/m^3 to 16.1 kN/m^3. The face failure feature is observed by gradually reducing the applied pressures, and the limit face pressure p_f is obtained when the horizontal displacement of tunnel face suddenly increases. A summary of 12 test results are given in Table 1 (Chambon and Corté 1994).

Table 1. A summary of centrifuge testing data from (Chambon and Corté 1994)

D(m)	*C*/*D*	γ (kN/m^3)	p_f(kPa)	$\mu_{G(x)}$[a](kPa)	$\sigma_{G(x)}$[a](kPa)
5	0.5	16.1	3.6	3.137	1.613
5	0.5	15.3	4.2	2.873	1.613
5	0.5	16.1	3.3	3.189	1.627
5	1	16.1	3.5	3.131	1.606
5	1	15.3	5.5	2.892	1.614
5	1	16.1	3.0	3.166	1.626
5	1	16.1	3.3	3.160	1.631
5	2	15.3	4.2	2.832	1.606
5	2	16.1	4.0	3.166	1.610
10	1	16.0	7.4	8.976	1.733
10	2	16.0	8.0	8.992	1.748
10	4	16.0	8.2	8.995	1.713

[a] $\mu_{G(x_i)}$ and $\sigma_{G(x_i)}$ are computed by the Mollon's model.

3. Bayesian characterization of model uncertainties

3.1 Model uncertainties

Denote $p = g(\boldsymbol{\theta}, \boldsymbol{\xi})$ a predictive model of necessary face pressures, $\boldsymbol{\theta}$ representing a vector of uncertain input parameters and $\boldsymbol{\xi}$ a vector of known model parameters (say *D*, *C*/*D*, γ in Table 1). The model uncertainty ε is defined as the difference between the model prediction *p* and the real system response *r*,

$$r = p + \varepsilon \tag{1}$$

The observed response *d* may not be exactly equal to the real system response *r* due to the observational uncertainty Δ. In this study, the limit face pressures p_f obtained in centrifuge tests in Table 1 are taken as the observed values, thus Δ is mainly attributed to the experimental test uncertainty. The observed response *d* can be written as,

$$d = r + \Delta \tag{2}$$

Substituting Eq.(1) to Eq.(2) leads to,

$$d = g(\boldsymbol{\theta}, \boldsymbol{\xi}) + \Delta + \varepsilon \tag{3}$$

In order to investigate the model uncertainty ε, a function $G(\boldsymbol{x}) = g(\boldsymbol{\theta}, \boldsymbol{\xi}) + \Delta$ is defined, where $\boldsymbol{x}$ =($\boldsymbol{\theta}$, Δ). Eq. (3) can be rewritten as,

$$d = G(\boldsymbol{x}) + \varepsilon \tag{4}$$

3.2 Bayesian estimations of model uncertainties

It is assumed that the model uncertainty ε follows a normal distribution with mean μ_ε and standard deviation σ_ε,

$$f(\varepsilon|\mu_\varepsilon, \sigma_\varepsilon) = \frac{1}{\sqrt{2\pi}\sigma_\varepsilon} exp\left[-\frac{(\varepsilon - \mu_\varepsilon)^2}{2{\sigma_\varepsilon}^2}\right] \tag{5}$$

The observational model response *d* is therefore described by a normal distribution with mean $G(\boldsymbol{x}) + \mu_\varepsilon$ and standard deviation σ_ε,

$$f(d|\mu_\varepsilon, \sigma_\varepsilon, \boldsymbol{x}) = \frac{1}{\sqrt{2\pi}\sigma_\varepsilon} exp\left[-\frac{(d - G(\boldsymbol{x}) - \mu_\varepsilon)^2}{2{\sigma_\varepsilon}^2}\right] \tag{6}$$

The physical model test results are used to calibrate the model uncertainties. Define d_i, $\boldsymbol{\theta}_i$, Δ_i represents the results of *i*-th physical model testing, i =1,…, *N*, *N* being the number of model tests. Assume that the *N* model tests are statistically independent, the likelihod function can be therefore derived as,

$$L(d|\mu_\varepsilon,\sigma_\varepsilon,\boldsymbol{x}) = \prod_{i=1}^{N} f(d_i|\mu_\varepsilon,\sigma_\varepsilon,\boldsymbol{x}_i) \tag{7}$$

Let $f(\mu_\varepsilon,\sigma_\varepsilon)$ and $f(\boldsymbol{x})$ represent the priori distributions of $(\mu_\varepsilon,\sigma_\varepsilon)$ and $\boldsymbol{x}$. According to the Bayes theorem, the posterior distribution $f(\mu_\varepsilon,\sigma_\varepsilon,\boldsymbol{x}|d)$ is expressed as (Bishop 2006, Pan et al. 2020),

$$f(\mu_\varepsilon,\sigma_\varepsilon,\boldsymbol{x}|d) = kf(\mu_\varepsilon,\sigma_\varepsilon)\times \prod_{i=1}^{N}\frac{1}{\sqrt{2\pi}\sigma_\varepsilon} exp\left[-\frac{(d_i - G(\boldsymbol{x}_i)-\mu_\varepsilon)^2}{2{\sigma_\varepsilon}^2}\right] f(\boldsymbol{x}_i) \tag{8}$$

where k is a normalization constant. In order to evaluate the statistics of ε, $\boldsymbol{x}$ in Eq.(8) can be eliminated by integration. However the integration computation is intractable due to the dimension issue of $\boldsymbol{x}_\mathrm{i}$ and the computational burden of $\mathrm{G}(\boldsymbol{x}_\mathrm{i})$, thus an approximation solution is given by (Zhang et al. 2009),

$$f(\mu_\varepsilon,\sigma_\varepsilon|d) \approx kf(\mu_\varepsilon,\sigma_\varepsilon)\times \prod_{i=1}^{N}\frac{1}{\sqrt{2\pi}(\sigma_\varepsilon^2+\sigma_{G(\boldsymbol{x}_i)}^2)} exp\left[-\frac{(d_i-\mu_{G(\boldsymbol{x}_i)}-\mu_\varepsilon)^2}{2(\sigma_\varepsilon^2+\sigma_{G(\boldsymbol{x}_i)}^2)}\right] \tag{9}$$

where $\mu_{\mathrm{G}(\boldsymbol{x}_\mathrm{i})}$ and $\mu_{\mathrm{G}(\boldsymbol{x}_\mathrm{i})}$ respectively represent the mean and standard deviation of $G(\boldsymbol{x})$ under the priori distribution of $f(\boldsymbol{x})$. The values of $\mu_{\mathrm{G}(\boldsymbol{x}_\mathrm{i})}$ and $\sigma_{\mathrm{G}(\boldsymbol{x}_\mathrm{i})}$ can be obtained by Monte Carlo simulations (MCS). The posterior distributions $f(\mu_\varepsilon,\sigma_\varepsilon|d)$ are obtained numerically by means of the shuffled complex evolution Metropolis algorithm because of its robustness and efficiency, a variant of Markov Chain Monte Carlo simulation proposed by (Vrugt et al. 2003).

4. Results

4.1 Priori distributions of model uncertainties and soil strength parameters

In this study, the priori distributions $f(\mu_\varepsilon)$ and $f(\sigma_\varepsilon)$ are respectively assumed to normally distributed and log-normally distributed. Based on the priori distributions, the statistics of model uncertainties can be expressed as (Zhang et al. 2009),

$$E(\varepsilon) = E(\mu_\varepsilon) \tag{10}$$

$$Var(\varepsilon) = Var(\mu_\varepsilon) + E^2(\sigma_\varepsilon) + Var(\sigma_\varepsilon) \tag{11}$$

The test uncertainty in centrifuge testing mainly includes systematic bias and random test error (Zhang et al. 2008, Zhang et al. 2009). In this study the systematic bias is neglected, which means that the mean of Δ is taken to be zero; the random test error is characterized by the standard deviation of Δ (Zhang et al. 2009). The standard deviation of Δ is firstly set to zero in the following analysis and its influence will be discussed later.

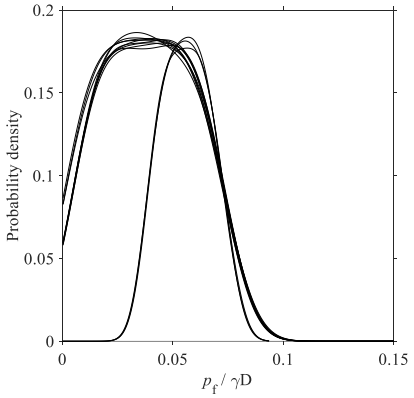

Figure 1. Obtained distributions of G(***x***) for 12 prototype tunnels using Mollon's model (Std(Δ) = 0)

As reported by Chambon and Corté (1994), the measurements of internal friction angle φ and cohesion c are subjected to some uncertainties, with φ in the range of 38-42 °and c in the range of 0-5kPa bounding the experimental values, thus they are modeled as random variables, namely $\boldsymbol{\theta}$**={***c*, φ**}.** Both φ and c are assumed to follow uniform distributions under the above bounds. According to the priori distributions of φ and c, the statistics of $G(\boldsymbol{x}_i)$ is firstly computed by MCS. Fig. 1 shows the obtained probability density distributions of $G(\boldsymbol{x}_i)$ (limit face pressure normalized by soil unit weight and tunnel diameter) for the 12 prototype tunnels using Mollon's model. The obtained values of $\mu_{\mathrm{G}(\mathrm{x_i})}$ and $\sigma_{\mathrm{G}(\mathrm{x_i})}$ are provided in Table 1.

4.2 Posterior model uncertainties

With the results of $\mu_{\mathrm{G}(\mathrm{x_i})}$ and $\sigma_{\mathrm{G}(\mathrm{x_i})}$, the prior knowledge of μ_ε and σ_ε, the posterior distributions of μ_ε and σ_ε can be obtained using the shuffled complex evolution Metropolis algorithm. Fig. 2 plots the posterior marginal density curves of μ_ε and σ_ε obtained from 1.0×10^4 Markov chain samples.

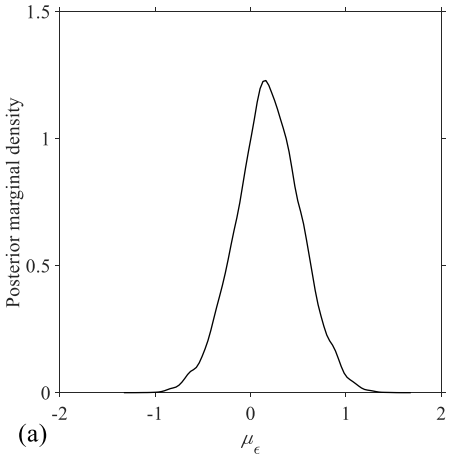

(a)

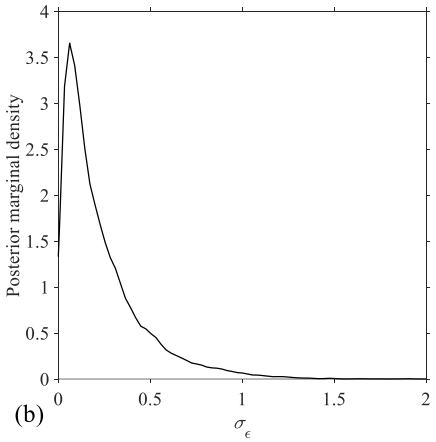

Figure 2. Posterior marginal distributions of (a) μ_ε and (b) σ_ε using Mollon's model (Std(Δ) = 0)

Table 2 presents the prior and the associated posterior statistics of μ_ε, σ_ε and ε using Eq.(10) and Eq.(11) for three considered predictive models. The posterior mean of model uncertainty $E(\varepsilon)$ for the Mollon's model and Soubra's model are positive, indicating that these two models underestimate the limit face pressures on the average. This confirms well the fact that these two models are based on the kinematical approach of limit analysis which provides a lower-bound estimate to the limit loads against resisting tunnel face failure. Besides, Mollon's model has the minimum magnitude of posterior mean $E(\varepsilon)$, implying that the Mollon's model is less biased than the other two. On the contrary, the Horn' model overestimates the limit face pressures since it has a negative posterior $E(\varepsilon)$. This indicates that the Horn's model tends to be conservative when estimating limit face pressures, which is preferred by engineers. However, the Horn's model has the largest posterior standard deviation Std(ε), which is fourteen times larger than those of the Mollon's model and Soubra's model.

Table 2. Priori and posterior statistics of model uncertainties (Std(Δ) = 0)

		μ_ε		σ_ε		ε	
		$E(\mu_\varepsilon)$	Std(μ_ε	$E(\sigma_\varepsilon)$	Std(σ_ε)	$E(\varepsilon)$	Std(ε)
Prior		0	0.5	0.5	1.0	0	1.225
Post	Mollon	0.179	0.346	0.242	0.262	0.179	0.482
erior	Soubra	0.899	0.349	0.259	0.255	0.899	0.490
	Horn	-0.328	0.502	5.618	1.659	-0.328	7.063

4.3 Influence of Std(Δ) = 0

In order to check the influence of Std(Δ) on the model uncertainty, the posterior statistics, E(ε) and Std(ε), are computed by varying Std(Δ) from 0.0 to 0.3. Fig. 3 shows the posterior statistics, E(ε) and Std(ε), as a function of Std(Δ) for the considered three models. It is seen that the Std(Δ) has negligible influences on E(ε) and Std(ε).

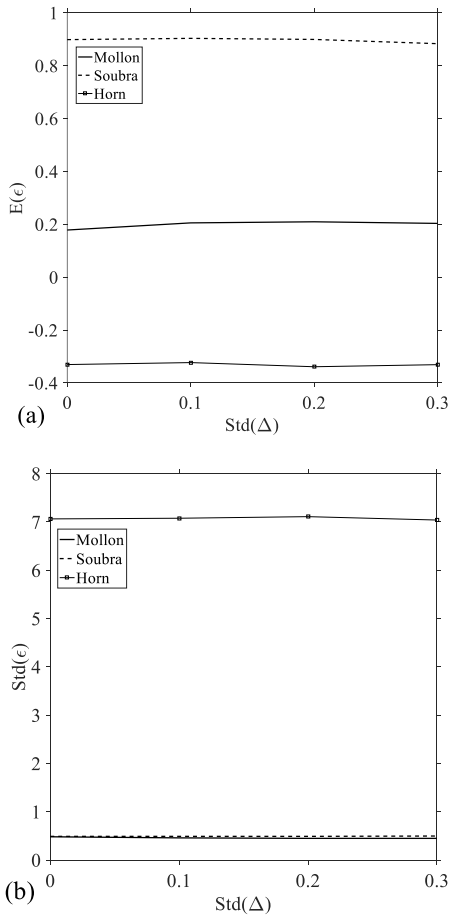

Figure 3. Effect of Std(Δ) on (a) posterior mean E(ε) and posterior standard deviation Std(ε)

5. Conclusions

This paper presents a study of applying Bayesian method to calibrate the model uncertainties of one LEM model (Horn model) and two LAM models (Mollon's model and Soubra's model) of predicting limit face pressures in frictional soils, by using 12 centrifuge model testing results and incorporating the test uncertainties and parameter uncertainties. The obtained results can be summarized as follows:

1. The posterior mean of model uncertainty for the two LAM models are positive, indicating that these two models underestimate the limit face pressures.
2. The Mollon's model is less biased than the other two models.
3. The Horn's model tends to be conservative estimating limit face pressures, but its model uncertainty has the largest posterior standard deviation.
4. The test uncertainty hardly affects the posterior statistics of model uncertainty.

References

Anagnostou, G., and Kovári, K. 1994. The face stability of slurry-shield-driven tunnels. *Tunnelling and underground space technology*, 9(2), 165-174.

Bishop, C. M. 2006. Pattern recognition and machine learning. Springer.

Chambon, P., and Corte, J. F. 1994. Shallow tunnels in cohesionless soil: stability of tunnel face. *Journal of Geotechnical Engineering*, 120(7), 1148-1165.

Chen, R. P., Li, J., Kong, L. G., and Tang, L. J. 2013. Experimental study on face instability of shield tunnel in sand. *Tunnelling and Underground Space Technology*,33, 12-21.

Idinger, G., Aklik, P., Wu, W., and Borja, R. I. 2011. Centrifuge model test on the face stability of shallow tunnel. *Acta Geotechnica*, 6(2), 105-117.

Kamata, H., and Mashimo, H. 2003. Centrifuge model test of tunnel face reinforcement by bolting.*Tunnelling and Underground Space Technology*, 18(2), 205-212.

Lü, X., Zhou, Y., Huang, M., and Zeng, S. 2018. Experimental study of the face stability of shield tunnel in sands under seepage condition. *Tunnelling and Underground Space Technology*, 74, 195-205.

Mollon, G., Dias, D., and Soubra, A. H. 2009. Probabilistic analysis and design of circular tunnels against face stability. *International Journal of Geomechanic*s, 9(6), 237-249.

Mollon, G., Dias, D., and Soubra, A. H. 2011. Rotational failure mechanisms for the face stability analysis of tunnels driven by a pressurized shield. *International Journal for Numerical and Analytical Methods in Geomechanics*, 35(12), 1363-1388.

Phoon, K. K., and Kulhawy, F. H. 2005. Characterisation of model uncertainties for laterally loaded rigid drilled shafts. *Geotechnique*, 55(1), 45-54.

Pan Q, Qu X, Liu L, Dias D. 2020. A sequential sparse polynomial chaos expansion using Bayesian regression for geotechnical reliability estimations. *International Journal for Numerical and Analytical Methods in Geomechanics*. 1–16. https://doi.org/10.1002/nag.3044

Soubra, A. H., Dias, D., Emeriault, F., and Kastner, R. 2008. Three-dimensional face stability analysis of circular tunnels by a kinematical approach. *In GeoCongress 2008: Characterization, Monitoring, and Modeling of GeoSystems*, Louisiana, March 9-12, 2008. ASCE, New Orleans, pp. 894-901.

Tang, C., and Phoon, K. K. 2018. Evaluation of model uncertainties in reliability-based design of steel H-piles in axial compression. *Canadian Geotechnical Journal*, 55(11), 1513-1532.

Tang, C., and Phoon, K. K. 2019. Characterization of model uncertainty in predicting axial resistance of piles driven into clay. *Canadian Geotechnical Journal*, 56(8), 1098-1118.

Vrugt, J. A., Gupta, H. V., Bouten, W., and Sorooshian, S. 2003. A Shuffled Complex Evolution Metropolis algorithm for optimization and uncertainty assessment of hydrologic model parameters. *Water Resources Research*, 39(8).

Zhao, L., Li, D., Yang, F., Li, L., and Cheng, X. 2019. Dimensionless parameter diagrams for the active and passive stability of a shallow 3D tunnel face. *KSCE Journal of Civil Engineering*, 23(2), 866-878.

Zhang, L. L., Zhang, L. M., and Tang, W. H. 2008. Similarity of soil variability in centrifuge models. *Canadian Geotechnical Journal*, 45(8), 1118-1129.

Zhang, J., Zhang, L. M., and Tang, W. H. 2009. Bayesian framework for characterizing geotechnical model uncertainty. *Journal of Geotechnical and Geoenvironmental Engineering*, 135(7), 932-940.

Zhang, D. M., Phoon, K. K., Huang, H. W., and Hu, Q. F. 2015. Characterization of model uncertainty for cantilever deflections in undrained clay. *Journal of Geotechnical and Geoenvironmental Engineering*, 141(1), 04014088.

Zizka, Z. 2019. Stability of a slurry supported tunnel face considering the transient support mechanism during excavation in non-cohesive soil. *PhD thesis*, Bochum University, Germany.